Biophysical Journal, Volume *115*

Supplemental Information

Molecular Determinants of Substrate Affinity and Enzyme Activity of a Cytochrome $P450_{BM3}$ Variant

Inacrist Geronimo, Catherine A. Denning, David K. Heidary, Edith C. Glazer, and Christina M. Payne

Table S1. Predicted protonation states of substrates at physiological pH.[a]

Substrate	Number of titratable atoms	Strongest acidic/basic pK_a	Charge at pH 7.4
diclofenac	2	4.00	-1.00
naproxen	1	4.19	-1.00
warfarin	1	5.56	-0.99
lovastatin	1	14.91	0.00
dextromethorphan	1	9.85	1.00
MDMA	1	10.14	1.00
astemizole	2	8.73	1.02
nicotine	2	8.58	0.94
cotinine	2	4.79	0.00
metyrapone	2	4.87	0.00

[a] https://chemicalize.com (accessed April 2018)

Table S2. Van der Waals component of pairwise interaction energy (kcal/mol) for diclofenac (DIF), naproxen (NPS), *S*-warfarin (SWF), *R*-warfarin (RWF), and lovastatin (LVA) complexes. Mean and standard deviation were calculated by averaging over 5-ns blocks.

Residue	DIF	NPS	SWF	RWF	LVA
S72	0.14 ± 0.57	1.02 ± 0.20	-0.54 ± 0.12	-0.18 ± 0.15	-0.76 ± 0.25
A74	-1.23 ± 0.20	-0.44 ± 0.08	-1.17 ± 0.04	-0.77 ± 0.17	-1.18 ± 0.36
L75	-4.20 ± 0.72	-3.60 ± 0.16	-4.05 ± 0.14	-2.67 ± 0.15	-3.99 ± 0.18
V78	-0.98 ± 0.10	-0.15 ± 0.01	-1.04 ± 0.05	-3.86 ± 0.20	-1.64 ± 0.12
V87	-2.50 ± 0.32	-1.71 ± 0.22	-3.01 ± 0.10	-2.19 ± 0.21	-2.11 ± 0.13
L181	-0.63 ± 0.33	-0.05 ± 0.02	-0.08 ± 0.01	-0.96 ± 0.04	-1.29 ± 0.15
T260	-0.15 ± 0.01	-0.06 ± 0.01	-0.08 ± 0.01	-1.31 ± 0.27	-0.48 ± 0.13
I263	-1.21 ± 0.24	-0.27 ± 0.08	-0.19 ± 0.03	-2.07 ± 0.10	-1.31 ± 0.15
A264	-1.52 ± 0.22	-1.10 ± 0.16	-0.92 ± 0.06	-2.06 ± 0.28	-1.21 ± 0.08
V267	-0.73 ± 0.08	-0.41 ± 0.21	-0.38 ± 0.07	-0.73 ± 0.08	-1.05 ± 0.30
T268	-0.93 ± 0.07	-0.79 ± 0.09	-0.82 ± 0.02	-0.58 ± 0.07	-1.25 ± 0.12
A328	-0.55 ± 0.42	-1.50 ± 0.07	-1.62 ± 0.21	-1.21 ± 0.21	-1.04 ± 0.17
A330	-0.47 ± 0.25	-1.89 ± 0.04	-1.33 ± 0.03	-0.50 ± 0.11	-2.91 ± 0.19
M354	-0.09 ± 0.04	-0.93 ± 0.06	-0.33 ± 0.09	-0.05 ± 0.01	-1.24 ± 0.07
L437	-3.37 ± 0.64	-1.64 ± 0.17	-3.79 ± 0.13	-3.76 ± 0.10	-4.99 ± 0.54
T438	-2.32 ± 0.42	-1.26 ± 0.11	-0.94 ± 0.04	-2.47 ± 0.30	-3.30 ± 0.36

Table S3. Van der Waals component of pairwise interaction energy (kcal/mol) for dextromethorphan (DEX), MDMA, and astemizole (AST) complexes. Mean and standard deviation were calculated by averaging over 5-ns blocks.

Residue	DEX	MDMA[a]	MDMA[b]	AST[a]	AST[b]	AST[c]
S72	-0.01 ± 0.01	-0.64 ± 0.11	-0.19 ± 0.03	-0.20 ± 0.11	-1.71 ± 0.90	-0.70 ± 0.52
A74	-0.04 ± 0.01	-0.15 ± 0.02	-0.88 ± 0.07	-0.59 ± 0.12	-0.97 ± 0.63	-1.13 ± 0.46
L75	-1.48 ± 0.19	-2.24 ± 0.14	-2.02 ± 0.11	-1.48 ± 0.42	-3.86 ± 1.10	-2.40 ± 0.82
V78	-1.34 ± 0.27	-0.06 ± 0.01	-0.99 ± 0.11	-5.41 ± 0.38	-2.15 ± 0.40	-2.76 ± 0.45
V87	-3.78 ± 0.08	-1.22 ± 0.16	-2.06 ± 0.18	-1.82 ± 0.12	-5.37 ± 0.37	-3.22 ± 0.40
L181	-1.17 ± 0.34	-0.02 ± 0.01	-0.17 ± 0.06	-3.20 ± 0.41	-0.58 ± 0.29	-1.05 ± 0.16
T260	-2.20 ± 0.15	-0.04 ± 0.01	-0.13 ± 0.02	-1.71 ± 0.09	-0.27 ± 0.03	-1.12 ± 0.22
I263	-3.88 ± 0.45	-0.10 ± 0.01	-0.70 ± 0.18	-4.65 ± 0.32	-1.45 ± 0.29	-2.80 ± 0.34
A264	-1.35 ± 0.17	-0.83 ± 0.04	-1.71 ± 0.08	-3.02 ± 0.14	-1.73 ± 0.19	-2.53 ± 0.23
V267	-1.47 ± 0.55	-0.02 ± 0.01	-0.60 ± 0.14	-1.08 ± 0.09	-1.48 ± 0.53	-1.17 ± 0.08
T268	-1.59 ± 0.10	-1.10 ± 0.06	-1.12 ± 0.04	-1.54 ± 0.05	-1.37 ± 0.17	-1.15 ± 0.16
A328	-0.95 ± 0.21	-1.36 ± 0.05	-1.16 ± 0.34	-2.40 ± 0.09	-1.17 ± 0.25	-2.84 ± 0.53
A330	-0.12 ± 0.03	-2.39 ± 0.12	-0.38 ± 0.07	-1.57 ± 0.20	-0.57 ± 0.24	-1.25 ± 0.19
M354	0.00	-0.72 ± 0.05	-0.03 ± 0.01	-0.14 ± 0.03	-0.08 ± 0.05	-0.05 ± 0.01
L437	-2.33 ± 0.44	-2.65 ± 0.11	-1.94 ± 0.14	-5.22 ± 0.92	-2.60 ± 0.31	-3.86 ± 0.57
T438	-1.40 ± 0.28	-1.28 ± 0.03	-2.09 ± 0.08	-3.14 ± 0.11	-1.37 ± 0.21	-2.76 ± 0.61

[a] positioned for N-dealkylation
[b] positioned for O-dealkylation
[c] positioned for C–H hydroxylation

Table S4. Van der Waals component of pairwise interaction energy (kcal/mol) for nicotine (NCT), cotinine (CTN), and metyrapone (MYT) complexes. Mean and standard deviation were calculated by averaging over 5-ns blocks.

Residue	NCT	CTN	MYT
S72	-0.12 ± 0.04	-0.19 ± 0.05	-0.01 ± 0.01
A74	-0.04 ± 0.01	-0.10 ± 0.02	-0.04 ± 0.01
L75	-1.35 ± 0.16	-2.23 ± 0.10	-1.34 ± 0.09
V78	-0.07 ± 0.01	-0.40 ± 0.06	-1.40 ± 0.07
V87	-1.61 ± 0.12	-1.66 ± 0.05	-3.78 ± 0.08
L181	-0.04 ± 0.01	-0.08 ± 0.03	-0.91 ± 0.12
T260	-0.11 ± 0.01	-0.14 ± 0.02	-1.82 ± 0.04
I263	-0.41 ± 0.08	-1.11 ± 0.19	-2.91 ± 0.05
A264	-1.54 ± 0.06	-2.17 ± 0.17	-2.89 ± 0.07
V267	-0.11 ± 0.03	-0.20 ± 0.06	-1.15 ± 0.02
T268	-1.02 ± 0.03	-0.79 ± 0.19	-1.21 ± 0.03
A328	-1.77 ± 0.14	-1.78 ± 0.11	-0.68 ± 0.13
A330	-0.94 ± 0.15	-0.39 ± 0.04	-0.07 ± 0.01
M354	-0.05 ± 0.01	-0.02 ± 0.01	0.00
L437	-1.84 ± 0.23	-2.41 ± 0.20	-2.12 ± 0.08
T438	-1.55 ± 0.09	-1.60 ± 0.08	-1.46 ± 0.06

Table S5. Hydrogen bond occupancies of substrates.

Substrate	Residue	Occupancy (%)
diclofenac:O1	S72:OG	28
diclofenac:O2	S72:OG	12
naproxen:O1	S72:OG	98
naproxen:O1	S72:N	40
naproxen:O2	S332:N	87
naproxen:O2	K69:NZ	88
S-warfarin:O2	K69:NZ	73
MDMA:N	L437:O	61

Table S6. Hydrogen bond occupancies of heme propionate A oxygen atoms.

Substrate	Heme propionate O atom	Hydrogen bond donor	Occupancy (%)
dextromethorphan	O1A	K69:NZ	24
	O2A	K69:NZ	27
MDMA	O1A	K69:NZ	74
	O2A	MDMA:N	61
astemizole	O1A	K69:NZ	34
	O2A	K69:NZ	27
nicotine	O1A	K69:NZ nicotine:N	16 39
	O2A	nicotine:N	46
naproxen	O1A	N395:N	19
	O2A	N395:N	17
S-warfarin	O1A	K69:NZ	53
	O2A	K69:NZ	27

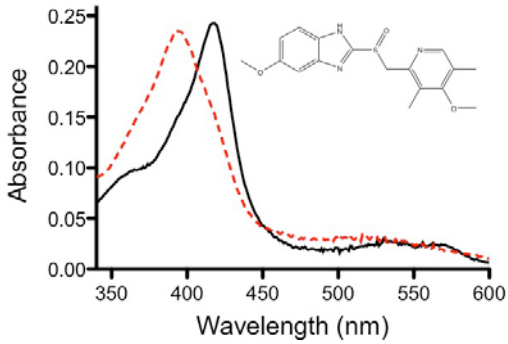

Figure S1. Absorption spectra of PM $P450_{BM3}$ bound to omeprazole (inset). The black solid curve indicates the resting, low spin state when water is bound to ferric iron. The red dotted curve represents the 100% high spin state in which water is no longer bound and omeprazole is in the active site.

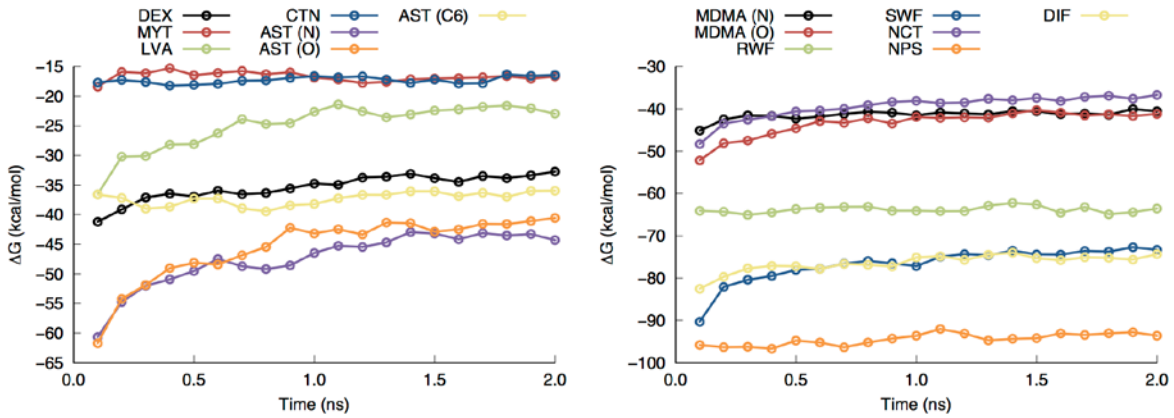

Figure S2. Gibbs free energy of the enzyme-substrate complexes during the last 2 ns of FEP/λ-REMD. The substrates are dextromethorphan (DEX), metyrapone (MYT), lovastatin (LVA), cotinine (CTN), astemizole (AST), MDMA, *R*-warfarin (RWF), *S*-warfarin (SWF), nicotine (NCT), naproxen (NPS), and diclofenac (DIF). Different binding poses were modeled for MDMA and astemizole, including N-dealkylation (N), O-dealkylation (O) and C–H hydroxylation (C6).

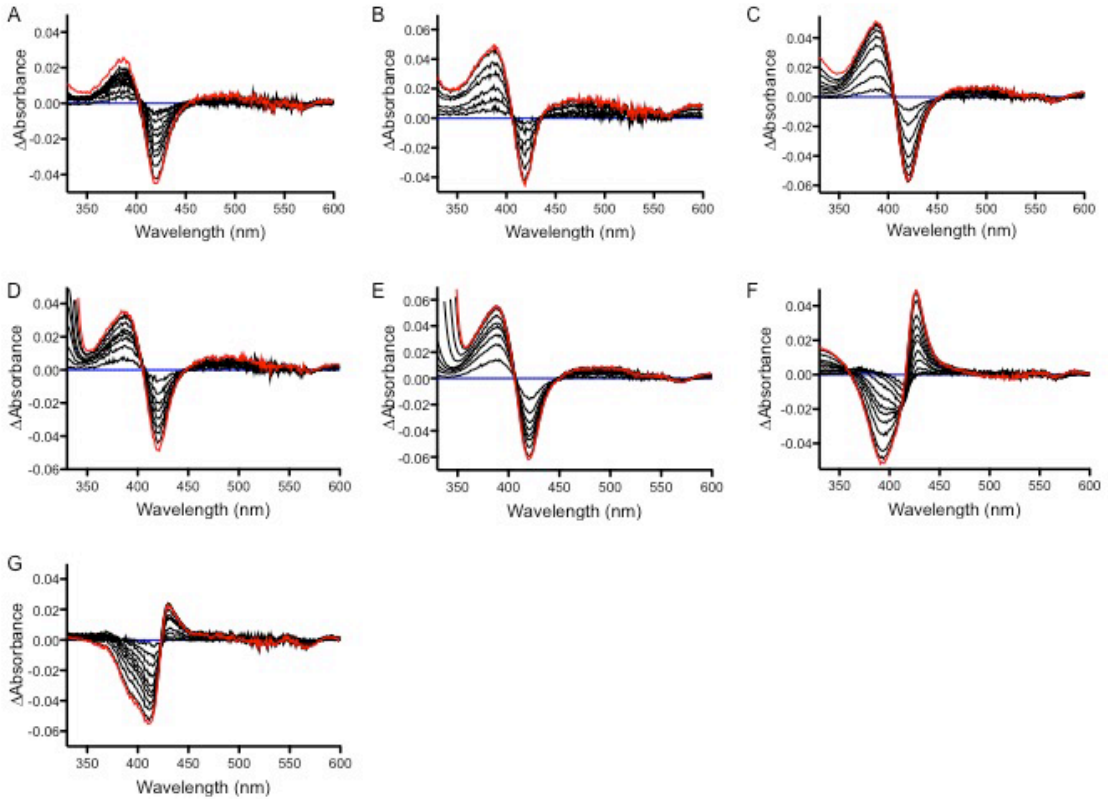

Figure S3. Difference spectra of all compounds bound to PM $P450_{BM3}$ studied experimentally. The blue line is PM $P450_{BM3}$ in which no compound is present, and the red line is fully saturated. (A) Dextromethorphan, (B) diclofenac, (C) lovastatin, (D) naproxen, and (E) racemic warfarin exhibit a type I spectral shift. (F) Cotinine and (G) nicotine exhibit a type II spectral shift.

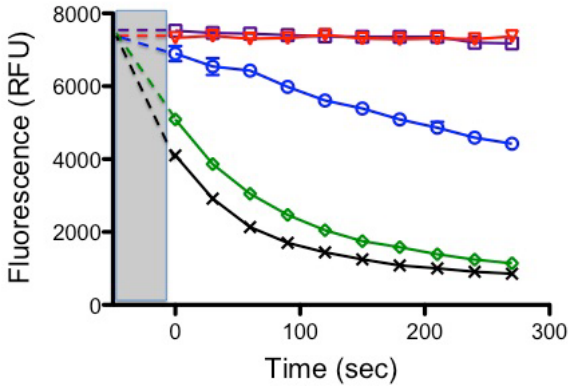

Figure S4. A 7-ethoxyresorufin-O-deethylase (EROD) activity assay was performed to determine if compounds that induced a type II spectral shift efficiently inhibited metabolism of the fluorescent substrate by PM $P450_{BM3}$. Fluorescence was monitored by excitation at 535 nm and emission at 595 nm. The gray box indicates the dead time of the instrument, and the dashed lines are projected emissions during that time (approximately 50 seconds). The black crosses indicate metabolism of 7-ethoxyresorufin when PM $P450_{BM3}$ was not inhibited. In contrast, the red triangles indicate the response when 7-ethoxyresorufin is not metabolized. Metyrapone-bound PM $P450_{BM3}$ (purple squares) was fully inhibited, whereas when cotinine was bound (green diamonds), activity was barely impacted. Interestingly, nicotine (blue circles) had an inhibitory effect on 7-ethoxyresorufin metabolism, but activity was still observed.

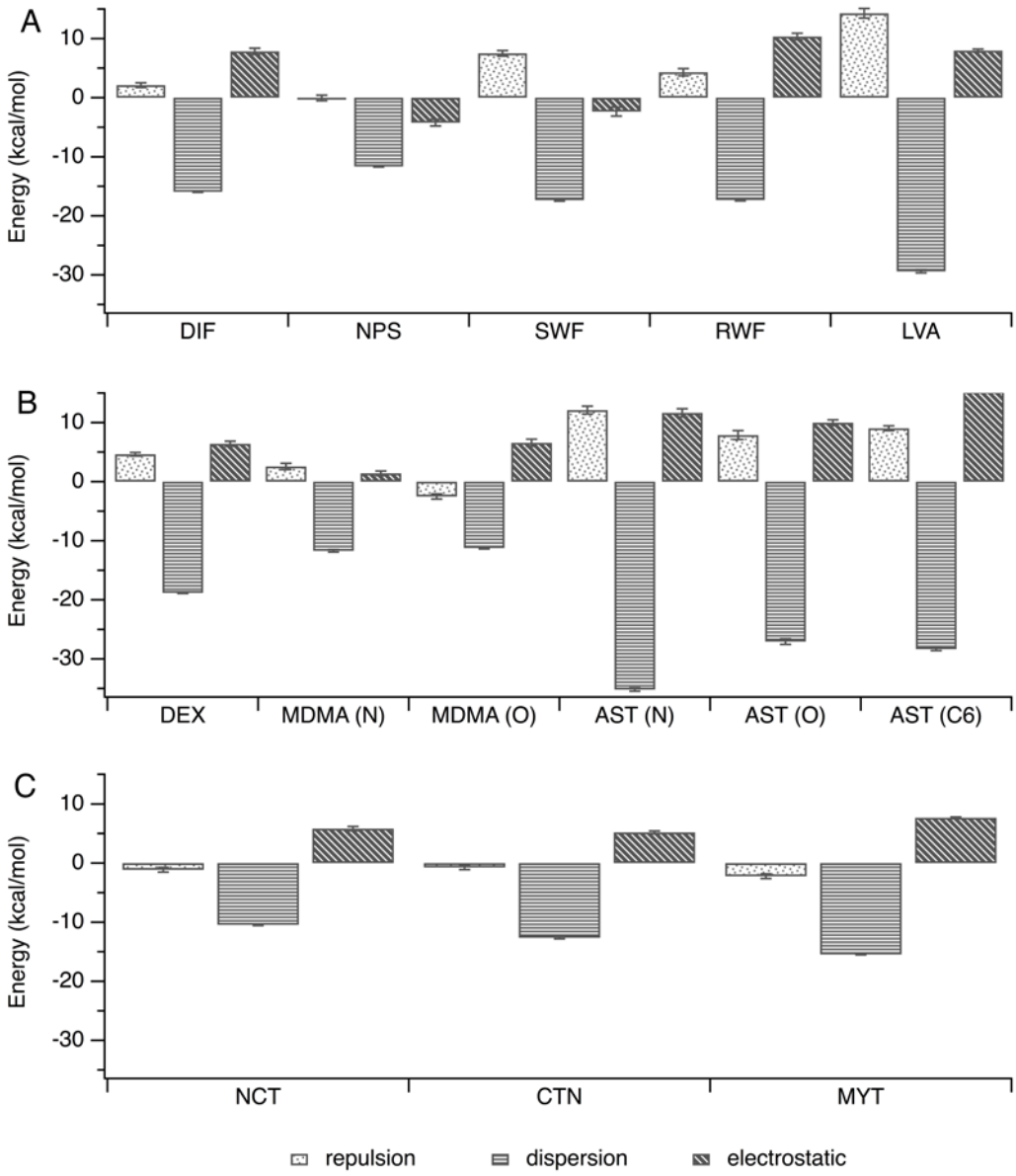

Figure S5. Repulsive, dispersive, and electrostatic energy contributions to the binding of (*A*) diclofenac (DIF), naproxen (NPS), *S*-warfarin (SWF), *R*-warfarin (RWF), lovastatin (LVA), (*B*) dextromethorphan (DEX), MDMA, astemizole (AST), (*C*) nicotine (NCT), cotinine (CTN), and metyrapone (MYT). Different binding poses were modeled for MDMA and astemizole, including N-dealkylation (N), O-dealkylation (O) and C–H hydroxylation (C6).

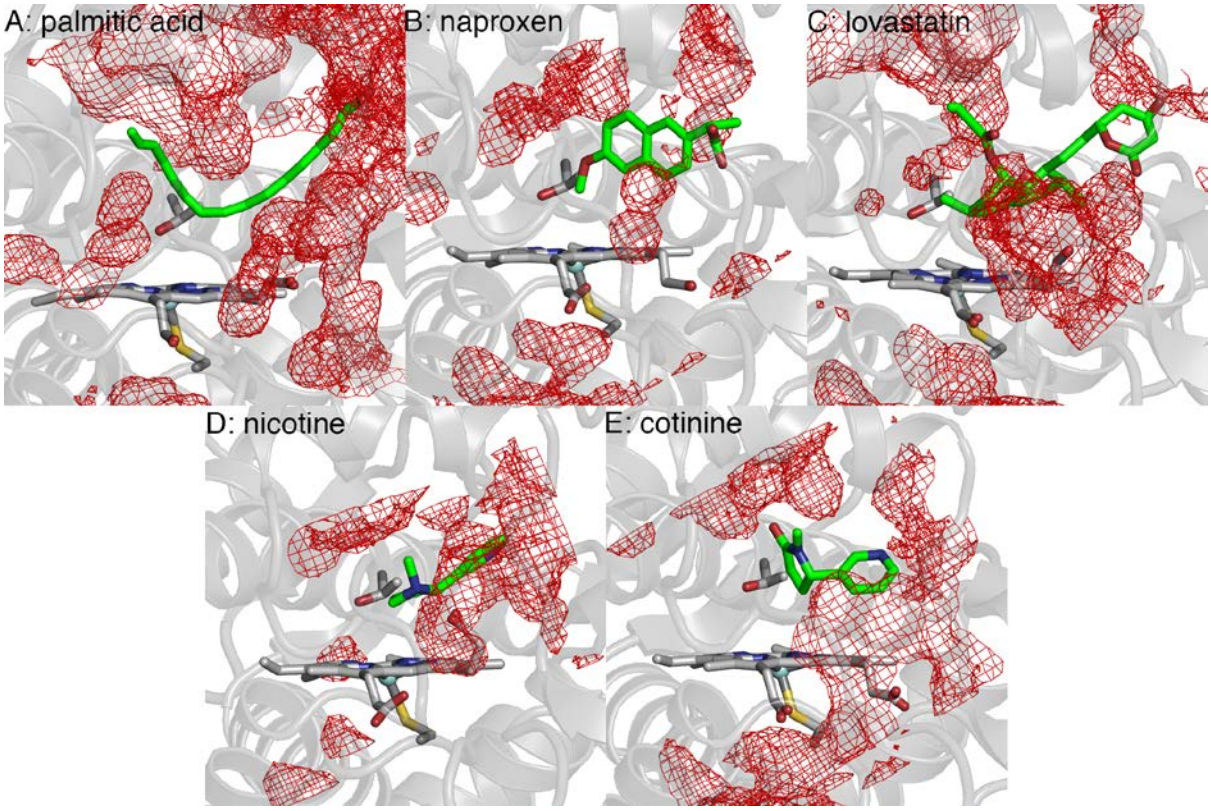

Figure S6. Water density at the PM $P450_{BM3}$ substrate channel, with the reference structure averaged from the MD simulation. T268, located at the distal side of the heme (helix I) and believed to play a role in proton delivery and oxygen activation, is also shown.

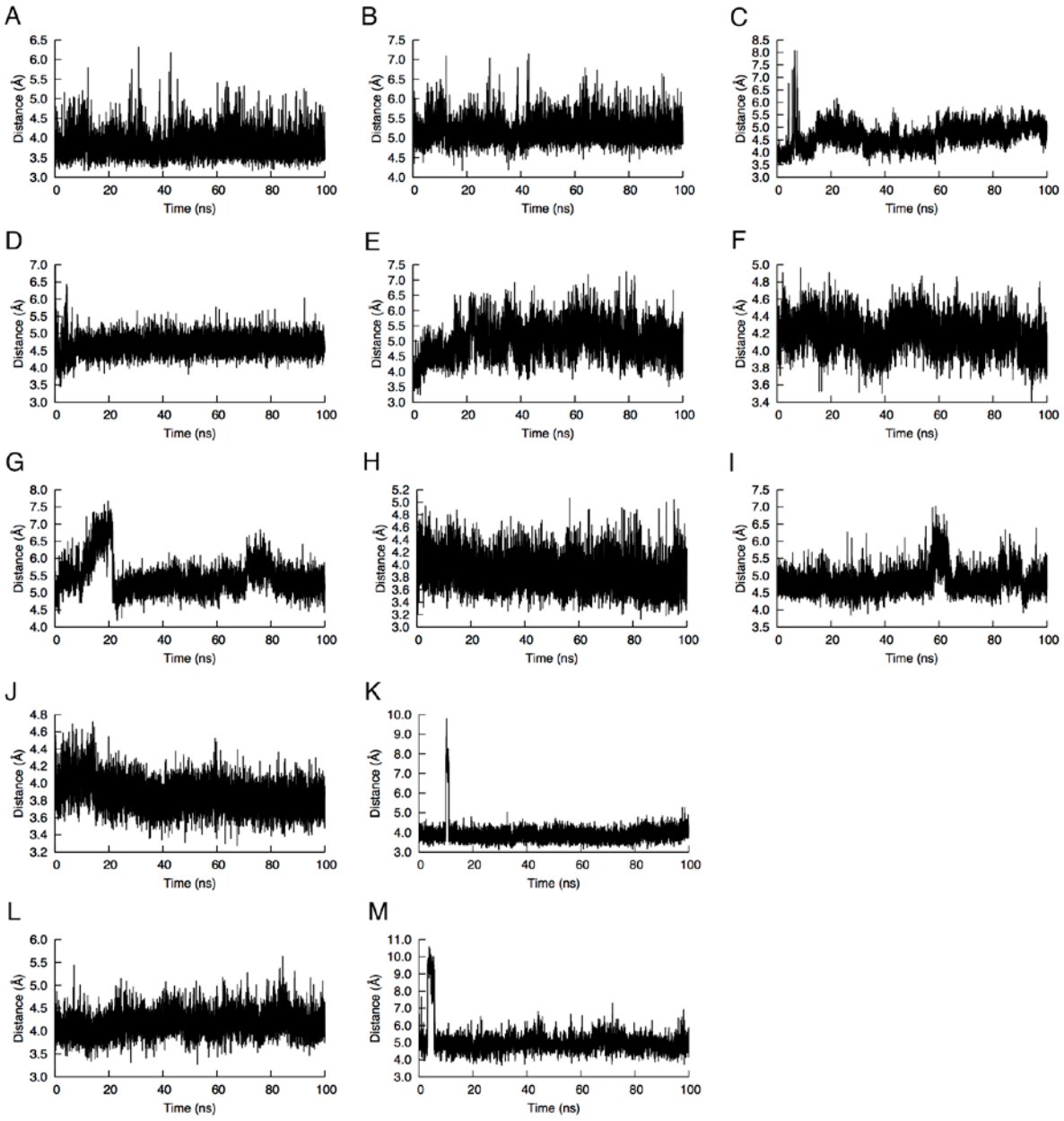

Figure S7. Plot of the distance between heme Fe and reacting atom of (*A*) diclofenac (C4'), (*B*) naproxen (methoxy C), (*C*) lovastatin (C6), (*D*) *S*-warfarin (C7), (*E*) *R*-warfarin (C4'), (*F*) dextromethorphan (protonated N), (*G–I*) astemizole (protonated N, methoxy C, C6), (*J*, *K*) MDMA (protonated N, C2), (*L*) nicotine (C5'), and (*M*) cotinine (C4').

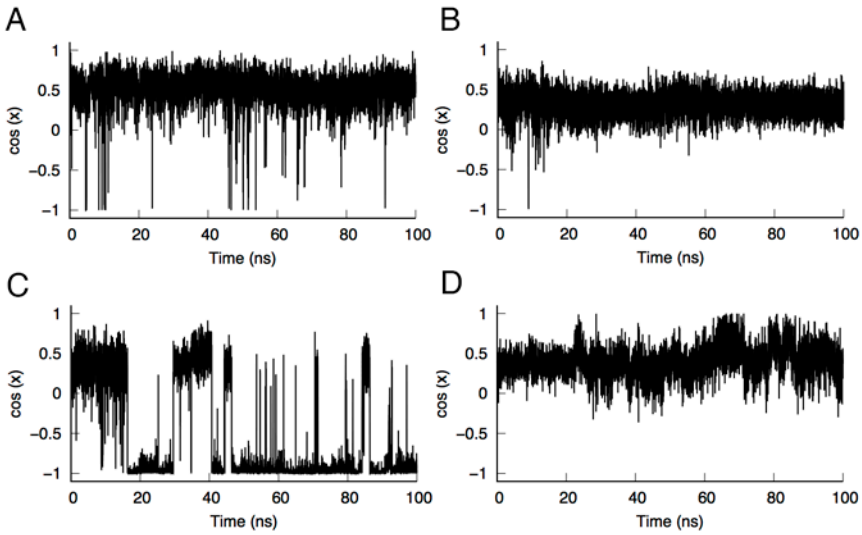

Figure S8. Plot of the cosine of the heme propionate A dihedral angle in (*A*) dextromethorphan, (*B*) MDMA, (*C*) astemizole, and (*D*) nicotine complexes of PM $P450_{BM3}$. The cosine of the dihedral angle in the PM-palmitic acid crystal structure (PDB ID: 4ZFB) is approximately -1.